

# Synthesis and Electrical Properties of Cation Deficient Perovskite-type Oxides in the Ln-A-Ti-Al-O System (Ln=La, Nd; A=Ca, Sr).

Sumio KATO\*, Yukio MATSUKI\*, Takahiro MARUYAMA\*, Yoshio MORIYA\*,

Mikio SUGAI\* and Shinichi NAKATA\*

\*Faculty of Engineering and Resource Science, Akita University  
1-1 Tegatagakuen-cho, Akita, 010-8502 Japan

E-mail : s\_kato@ipc.akita-u.ac.jp

E-mail : ymoriya@ipc.akita-u.ac.jp

E-mail : sugai@ipc.akita-u.ac.jp

E-mail : snakata@ipc.akita-u.ac.jp

The effects of ion vacancy on the crystal structure and the electrical conductivity of perovskite-type oxides were investigated. The cation and oxide ion deficient perovskite-type oxides  $\text{LnA}_{2-x}\text{Ti}_2\text{AlO}_{9-d}$  (Ln=La, Nd; A=Ca, Sr) were synthesized. Single-phase samples of  $\text{LnA}_{2-x}\text{Ti}_2\text{AlO}_{9-d}$  were prepared by heating at 1673 K in air in the compositional range of  $x=0-0.3$  for both A=Ca and Sr. The crystal structures were cubic perovskite-type for A=Sr and orthorhombic perovskite-type for A=Ca. Lattice parameters of  $\text{LnA}_{2-x}\text{Ti}_2\text{AlO}_{9-d}$  increased with increasing amounts of A cation vacancies. All the samples exhibited semiconducting behavior in the temperature range of 573-1023 K in air. The measurements of conductivity for  $\text{LnA}_{2-x}\text{Ti}_2\text{AlO}_{9-d}$  as a function of oxygen partial pressure revealed n-type conductivity at oxygen partial pressure less than 0.21 atm. The conductivities of  $\text{LnA}_{2-x}\text{Ti}_2\text{AlO}_{9-d}$  increased with increasing amount of A cation and oxide ion vacancies for both A=Ca and Sr.

**Key Words** : perovskite, crystal structure, cation vacancy, oxide ion conductor, electrical conductivity

## 1. Introduction

Oxide ion conductors have been developed for utilization as oxygen sensors and solid electrolytes for solid oxide fuel cells (SOFC). Some oxygen deficient perovskite type oxides exhibit oxide ion conduction and have conductivities comparable to stabilized zirconia. Recently, Yoshioka et al. reported that the perovskite-type oxides of La-Ti-Al-O system containing cation vacancy at the 12-fold coordinated site (A-site) exhibit oxide ion conduction [1]. This suggests that the introduction of cation vacancies into perovskite-type oxides is effective for imparting oxide ion conduction. In the perovskite-type lattice, A-site ions and oxide ions form a cubic closed packing structure as shown in Figure 1. Because the crystallographic environments of A-site and oxide ions are very similar, the vacancy at A-site would affect diffusion of oxide ions as well as the oxide ion vacancies.

Some perovskite-type oxides with cation vacancies are known, such as  $\text{La}_x\text{VO}_3$ ,  $\text{La}_{1/3}\text{NbO}_3$  and  $\text{La}_{1/3}\text{TaO}_3$  [2, 3]. Li ion doped  $\text{La}_{2/3}\text{TiO}_3$  has been studied on Li ion conduction [4, 5]. A few studies on oxide ion conductivity of cation deficient perovskite-type oxide have also been reported. In the present study, in order to clarify the effect of cation vacancy on oxide ion conductivity of perovskite-type oxides, the oxide ion and A-cation deficient perovskite-type oxides  $\text{LnA}_{2-x}\text{Ti}_2\text{AlO}_{9-d}$  (Ln=La, Nd; A=Sr, Ca)

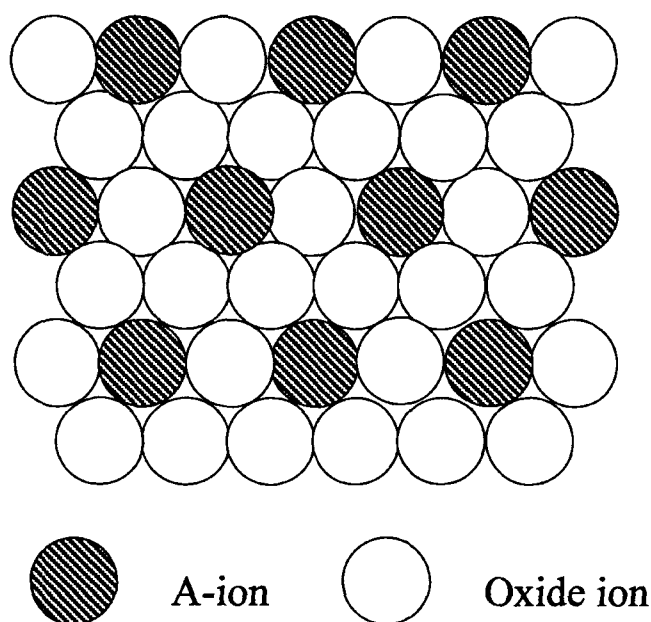


Figure 1 Arrangement of A-site and O ions in a cubic perovskite-type structure.

were synthesized and the electrical properties of these compounds were investigated.

## 2. Experimental

### 2.1 Sample Preparation

$\text{LnA}_{2-x}\text{Ti}_2\text{AlO}_{9-d}$  samples were synthesized by solid-state reaction. Powders of  $\text{CaCO}_3$ ,  $\text{SrCO}_3$ ,  $\text{Al}_2\text{O}_3$ ,  $\text{TiO}_2$ ,  $\text{Nd}_2\text{O}_3$  and  $\text{La}_2\text{O}_3$  were used as starting materials. Appropriate amounts of the powders were mixed by ball-mill in ethanol and pressed into pellets of 10 mm diameter at 100 MPa. The pellets were fired at 1673 K for 12 h in air. Reforming and firing were repeated several times.

### 2.2 Characterization

Phase identification was made by the powder X-ray diffraction (XRD) method using a diffractometer (Rigaku RAD-C). Lattice parameters of the compounds were determined by Rietveld analysis of the XRD data using the RIETAN program [6].

The ac conductivities of materials were obtained using two-probe impedance spectroscopy. The electrodes formed by applying silver paste and firing at 673 K. The measurements were performed with a LCR meter (Hewlett-Packard 4284 A) over a frequency range of 20 Hz to 1 MHz in the temperature range from 573 to 1023 K and oxygen partial pressure range from 0.21 to  $10^{-17}$  atm.

## 3. Results and Discussions

### 3.1 Synthesis

Sr and oxide ion deficient perovskite-type  $\text{LnSr}_{1.7}\text{Ti}_2\text{AlO}_{9-d}$  ( $\text{Ln}=\text{La}, \text{Nd}$ ) were synthesized at 1673 K for 48 h as single phases. Figure 2 shows the XRD patterns of  $\text{LaSr}_{2-x}\text{Ti}_2\text{AlO}_{9-d}$  and the lattice parameters of  $\text{LnSr}_{2-x}\text{Ti}_2\text{AlO}_{9-d}$  are given in Table 1. In the compositional range of  $x > 0.3$ , Al-containing oxides existed with the perovskite phases, which were  $\text{LaAl}_{11}\text{O}_{18}$  at  $x=0.7$  and  $\text{LaTi}_2\text{Al}_9\text{O}_{19}$  at  $x \geq 1.0$  for  $\text{Ln}=\text{La}$  and  $\text{Sr}_3\text{Al}_{32}\text{O}_{51}$  at  $x=0.7$ ,  $\text{SrTi}_2\text{Al}_6\text{O}_{19}$  at  $x \geq 1.0$  for  $\text{Ln}=\text{Nd}$ . Figure 3 shows the relationship between amount of Sr vacancy  $x$  and lattice parameter  $a$  for  $\text{LaSr}_{2-x}\text{Ti}_2\text{AlO}_{9-d}$ . Although perovskite-type phases with no impurities were obtained in the compositional region  $0 \leq x \leq 0.3$ , the lattice parameters of both  $\text{Ln}=\text{La}$  and  $\text{Nd}$  compounds increased with increasing  $x$  up to  $x=1.0$ . Thangadurai, et al. reported that the synthesis of oxygen-deficient perovskite-type  $\text{KM}_{1-x}\text{Al}_x\text{O}_{3-x}$  ( $\text{M}=\text{Nb}, \text{Ta}$ ) [7]. The lattice parameters of  $\text{KNb}_{0.5}\text{Al}_{0.5}\text{O}_{2.5}$ ,  $a=0.5693$  nm,  $b=0.5685$  nm,  $c=3.985$  nm were larger than those of  $\text{KNbO}_3$ ,  $a=0.5690$  nm,  $b=0.5664$  nm,  $c=3.969$  nm and that of  $\text{KTa}_{0.5}\text{Al}_{0.5}\text{O}_{2.5}$ ,  $a=0.3983$  nm is close to  $\text{KTaO}_3$ ,  $a=0.3989$  nm, although the ionic radius of  $\text{Al}^{3+}$  (0.0535 nm) is smaller than  $\text{Nb}^{5+}$  (0.064 nm) and  $\text{Ta}^{5+}$  (0.064 nm) [8]. These results are examples that introduction of oxygen vacancy leads to expansion of the perovskite-type. Therefore, expansion of the lattice with increasing  $x$  for  $\text{LaSr}_{2-x}\text{Ti}_2\text{AlO}_{9-d}$  would be due to increase amount of oxygen vacancy. The lattice parameters of  $\text{LaSr}_{2-x}\text{Ti}_2\text{AlO}_{9-d}$  were larger than those of  $\text{NdSr}_{2-x}\text{Ti}_2\text{AlO}_{9-d}$ . This result corresponds to larger ionic radius of  $\text{La}^{3+}$  (0.132 nm) than  $\text{Nd}^{3+}$  (0.127 nm).

Ca and oxide ion deficient orthorhombic perovskite-type oxides  $\text{LnCa}_{1.7}\text{Ti}_2\text{AlO}_{9-d}$  were synthesized at 1673 K for 36 h as a single phase. The XRD patterns of  $\text{LaCa}_{2-x}\text{Ti}_2\text{AlO}_{9-d}$  ( $\text{Ln}=\text{La}, \text{Nd}$ ) in air are shown in Figure 4 and the lattice parameters of  $\text{LnCa}_{2-x}\text{Ti}_2\text{AlO}_{9-d}$  are given in Table 1. In the ranges of  $x=0.7$  and  $x > 0.7$  for  $\text{Ln}=\text{La}$ , the Al-containing oxides  $\text{LaAl}_{11}\text{O}_{18}$  and  $\text{LaTi}_2\text{Al}_9\text{O}_{19}$

Table 1 Lattice parameters of  $\text{LnA}_{2-x}\text{Ti}_2\text{AlO}_{9-d}$  ( $\text{Ln}=\text{La}, \text{Nd}$ ;  $\text{A}=\text{Ca}, \text{Sr}$ )

Composition	$a/\text{nm}$	$b/\text{nm}$	$c/\text{nm}$
$\text{LaSr}_2\text{Ti}_2\text{AlO}_9$	0.38649(4)		
$\text{LaSr}_{1.7}\text{Ti}_2\text{AlO}_{8.7}$	0.38678(1)		
$\text{LaCa}_2\text{Ti}_2\text{AlO}_9$	0.54047(4)	0.76450(7)	0.54019(8)
$\text{LaCa}_{1.7}\text{Ti}_2\text{AlO}_{8.7}$	0.54138(6)	0.76481(4)	0.54135(5)
$\text{NdSr}_2\text{Ti}_2\text{AlO}_9$	0.38534(7)		
$\text{NdSr}_{1.7}\text{Ti}_2\text{AlO}_{8.7}$	0.38545(5)		
$\text{NdCa}_2\text{Ti}_2\text{AlO}_9$	0.53964(4)	0.76087(7)	0.53730(4)
$\text{NdCa}_{1.7}\text{Ti}_2\text{AlO}_{8.7}$	0.54006(5)	0.76196(8)	0.53844(5)
$\text{La}_{1.6}\text{Sr}_{1.1}\text{Ti}_2\text{AlO}_9$	0.38579(2)		
$\text{La}_{1.6}\text{Ca}_{1.1}\text{Ti}_2\text{AlO}_9$	0.54308(5)	0.76605(7)	0.54223(5)

existed with the perovskite-type phase, respectively. These results are similar to those for  $\text{A}=\text{Sr}$ . In the case of  $\text{Ln}=\text{Nd}$ , the XRD peaks of  $\text{Al}_2\text{O}_3$  and  $\text{CaTi}_3\text{Al}_{18}\text{O}_{18}$  were observed at  $x > 0.3$  and  $x \geq 1.0$ , respectively.

Figure 5 shows the compositional dependences of lattice parameters  $a$ ,  $b$  and  $c$  for  $\text{LaCa}_{2-x}\text{Ti}_2\text{AlO}_{9-d}$ . The lattice parameters  $a$ ,  $b$  and  $c$  increased with increasing amount of Ca vacancy  $x$  at  $0 \leq x \leq 1.3$ .

The relationship between the ionic radii and symmetry of

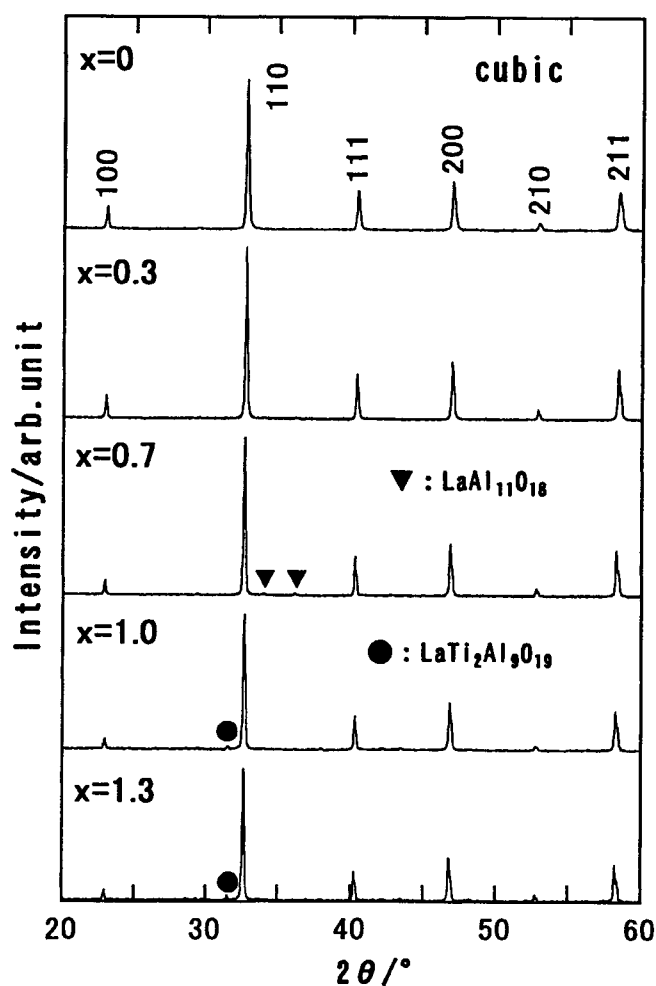


Figure 2 X-ray diffraction patterns of  $\text{LaSr}_{2-x}\text{Ti}_2\text{AlO}_{9-d}$  synthesized at 1673 K in air.

perovskite-type lattice can also be examined based on the tolerance factor [9] represented by Eq. (1).

$$t = (r_A + r_O) / \sqrt{2}(r_B + r_O) \quad (1)$$

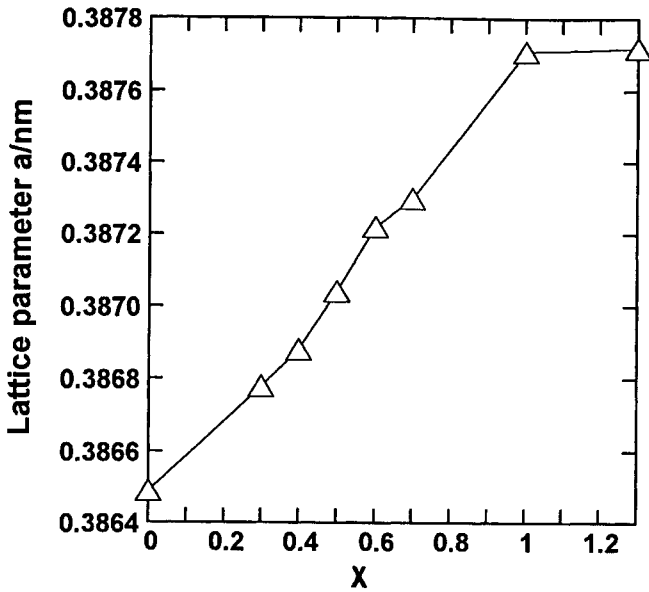


Figure 3 Relationship between composition and lattice parameters for  $\text{LaSr}_{2-x}\text{Ti}_2\text{AlO}_{9-d}$ .

$r_A$ ,  $r_B$  and  $r_O$  are the ionic radii of A, B and O, respectively. A and B cations occupy 12-fold coordinated and 6-fold coordinated sites in the cubic perovskite-type structure, respectively. In the case of  $t=1$ , the relationship among the ionic radii is ideal for forming cubic perovskite-type structure. When  $t$  decreases,

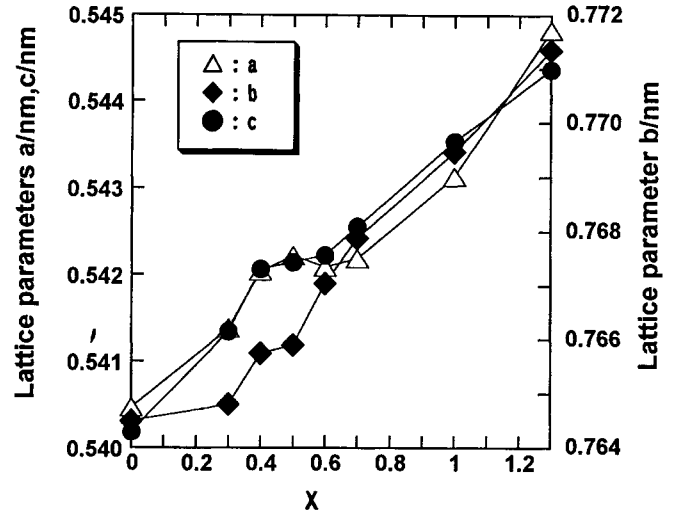


Figure 5 Relationship between composition and lattice parameters for  $\text{LaCa}_x\text{Ti}_2\text{AlO}_{9-d}$ .

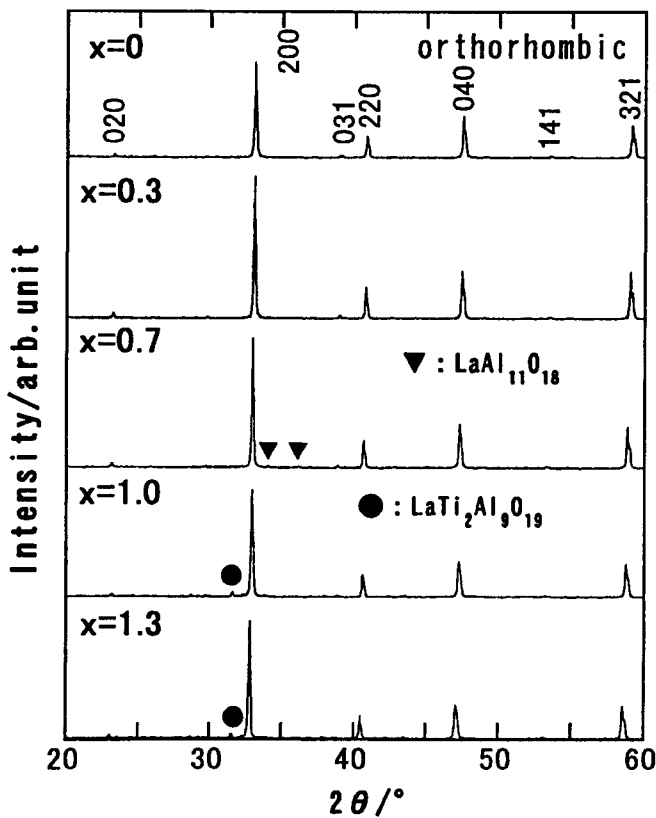


Figure 4 X-ray diffraction patterns of  $\text{LaCa}_{2-x}\text{Ti}_2\text{AlO}_{9-d}$  synthesized at 1673 K in air.

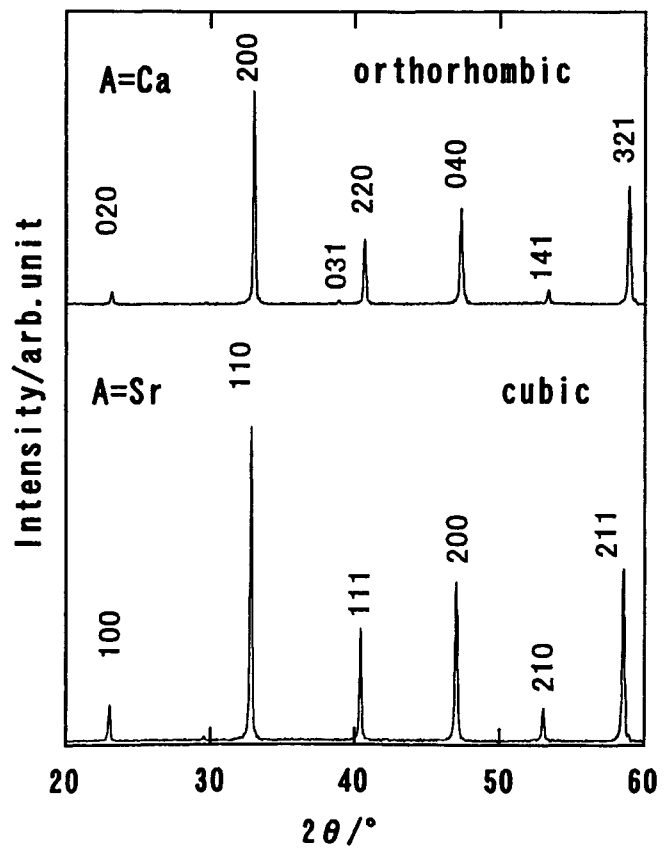


Figure 6 X-ray diffraction patterns of  $\text{La}_{1.6}\text{Sr}_{1.1}\text{Ti}_2\text{AlO}_9$  and  $\text{La}_{1.6}\text{Ca}_{1.1}\text{Ti}_2\text{AlO}_9$ .

distorted perovskite-type oxides that have an orthorhombic or a monoclinic symmetry tend to form. As the average ionic radius of ( $\text{Ln}^{3+}, \text{Ca}^{2+}$ ) that occupies the A site is smaller than that of ( $\text{Ln}^{3+}, \text{Sr}^{2+}$ ),  $t$  values for  $\text{LnCa}_{2-x}\text{Ti}_2\text{AlO}_{9-d}$  are smaller than those for  $\text{LnSr}_{2-x}\text{Ti}_2\text{AlO}_{9-d}$ . For example, the  $t$  values of  $\text{LaCa}_2\text{Ti}_2\text{AlO}_9$  and  $\text{LaSr}_2\text{Ti}_2\text{AlO}_9$  calculated using Shannon's ionic radii [8] are 0.98 and 1.00. Thus, formation of distorted perovskite-type compounds for  $\text{Ln}=\text{Nd}$  is explained by their smaller  $t$  values than those for  $\text{Ln}=\text{La}$ .

In order to clarify the effect of cation and oxide ion vacancies on conductivity separately, we attempted to synthesize Sr deficient  $\text{La}_{1.6}\text{Sr}_{1.1}\text{Ti}_2\text{AlO}_9$  and Ca deficient  $\text{La}_{1.6}\text{Ca}_{1.1}\text{Ti}_2\text{AlO}_9$  without oxygen vacancy. The XRD patterns of  $\text{La}_{1.6}\text{Sr}_{1.1}\text{Ti}_2\text{AlO}_9$  and  $\text{La}_{1.6}\text{Ca}_{1.1}\text{Ti}_2\text{AlO}_9$  are shown in Figure 6. These patterns show the presence of single phases with diffraction peaks that could be indexed to the cubic and orthorhombic cell for  $\text{La}_{1.6}\text{Sr}_{1.1}\text{Ti}_2\text{AlO}_9$  and  $\text{La}_{1.6}\text{Ca}_{1.1}\text{Ti}_2\text{AlO}_9$ , respectively.

### 3.2 Electrical conductivity

Figure 7 shows the temperature dependences of the conductivity ( $\sigma$ ) for  $\text{LaSr}_{2-x}\text{Ti}_2\text{AlO}_{9-d}$  in air. The relationships between  $\log \sigma$  and  $1/T$  indicate semiconducting behavior for  $\text{LaSr}_2\text{Ti}_2\text{AlO}_9$  and  $\text{LaSr}_{1.7}\text{Ti}_2\text{AlO}_{8.7}$ . The Sr and oxygen-deficient compounds  $\text{LaSr}_{1.7}\text{Ti}_2\text{AlO}_{8.7}$  exhibited higher conductivities than the stoichiometric compounds. The ionic transference number ( $t_i$ ) of  $\text{LaSr}_2\text{Ti}_2\text{AlO}_9$  and  $\text{LaSr}_{1.7}\text{Ti}_2\text{AlO}_{8.7}$ , which was estimated from electromotive force of the oxygen concentration cell, were 0.89 and 0.41 at 1073 K, respectively. This result suggests that the conductivities given in Figure 7 would be sums of oxide ionic and electronic (electron or hole) conductivities in the compounds. In order to determine the charge carrier that is the dominant contributor to the electrical conduction, oxygen partial pressure ( $P_{\text{O}_2}$ ) dependence of conductivity was investigated. In the low

oxygen partial pressure range, elimination of oxygen from the lattice occurs and generates electrons by the following reaction according to Eq. (2) written using Kröger-Vink notation.

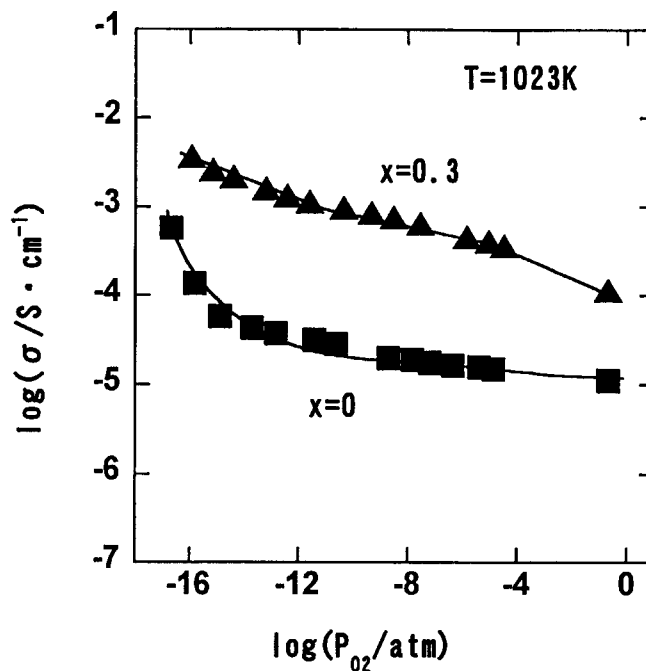
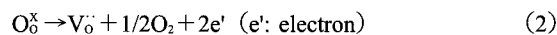


Figure 8 Electrical conductivity of  $\text{LaSr}_{2-x}\text{Ti}_2\text{AlO}_{9-d}$  as a function of oxygen partial pressure.

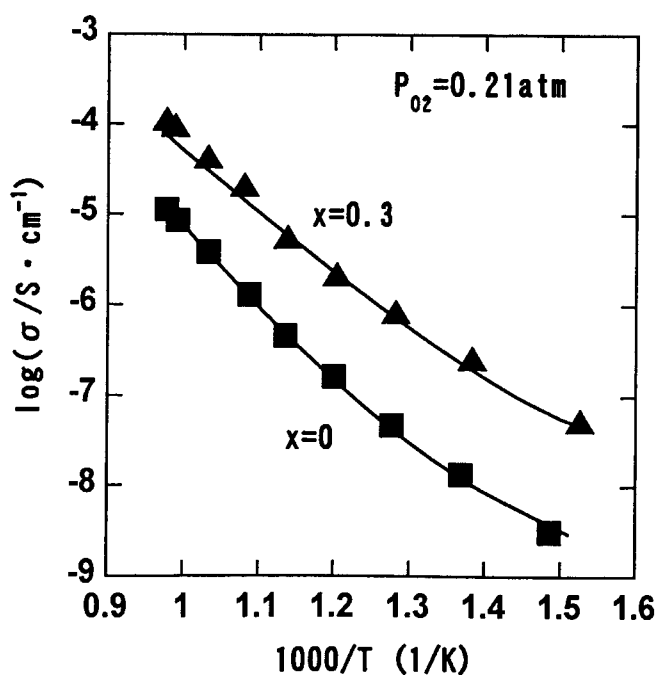


Figure 7 Electrical conductivity of  $\text{LaSr}_{2-x}\text{Ti}_2\text{AlO}_{9-d}$  as a function of temperature at  $P_{\text{O}_2}=0.21$  atm.

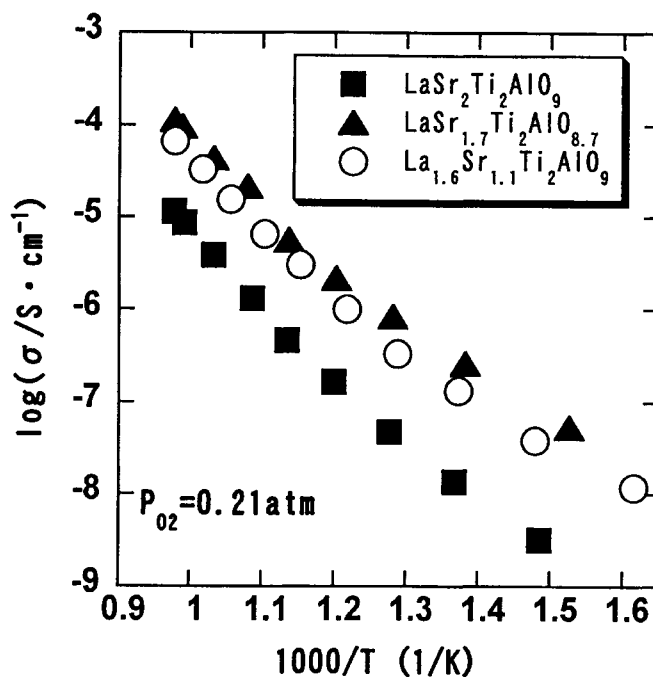


Figure 9 Electrical conductivity of  $\text{LaSr}_2\text{Ti}_2\text{AlO}_9$ ,  $\text{La}_{1.6}\text{Sr}_{1.1}\text{Ti}_2\text{AlO}_9$  and  $\text{LaSr}_{1.7}\text{Ti}_2\text{AlO}_{8.7}$  as a function of temperature at  $P_{\text{O}_2}=0.21$  atm.

$$K = [V_{\text{O}}^{\cdot\cdot}] n^2 P_{\text{O}_2}^{-1/2} \quad (3)$$

n : electron concentration

Therefore, the electron concentration will be expressed as Eq. (4)

$$n = K [V_{\text{O}}^{\cdot\cdot}]^{-1} P_{\text{O}_2}^{-1/4} \quad (4)$$

Because the concentration of  $V_{\text{O}}^{\cdot\cdot}$  is determined from the composition,  $[V_{\text{O}}^{\cdot\cdot}]$  is regarded as to be constant. The electrical conductivity of  $\text{LaSr}_{1.7}\text{Ti}_2\text{AlO}_{8.7}$  decreased with increasing  $P_{\text{O}_2}$ , indicating the presence of electron conduction. However, it did not obey  $-1/4$  power dependence of the oxygen partial pressure. According to the ionic transference numbers of  $\text{LaSr}_2\text{Ti}_2\text{AlO}_9$  and  $\text{LaSr}_{1.7}\text{Ti}_2\text{AlO}_{8.7}$ , the contribution of electronic conduction for  $\text{LaSr}_{1.7}\text{Ti}_2\text{AlO}_{8.7}$  is larger than that for  $\text{LaSr}_2\text{Ti}_2\text{AlO}_9$ . It appears that the higher conductivity of Sr and oxygen-deficient compounds is due to the enhancement of electronic conductivity. A comparison of the conductivities between stoichiometric  $\text{LaSr}_2\text{Ti}_2\text{AlO}_9$ , Sr deficient  $\text{La}_{1.6}\text{Sr}_{1.1}\text{Ti}_2\text{AlO}_9$  and Sr and oxide ion deficient  $\text{LaSr}_{1.7}\text{Ti}_2\text{AlO}_{8.7}$  is shown in Figure 9. The conductivity of  $\text{La}_{1.6}\text{Sr}_{1.1}\text{Ti}_2\text{AlO}_9$  is higher than that of  $\text{LaSr}_2\text{Ti}_2\text{AlO}_9$ , but slightly lower than that of  $\text{LaSr}_{1.7}\text{Ti}_2\text{AlO}_{8.7}$ . This result suggests that the introduction of Sr vacancy enhances electrical conductivity similarly to the introduction of oxygen vacancy.

#### 4. Conclusions

We have shown that it is possible to synthesize cation deficient perovskite  $\text{LnA}_{2-x}\text{Ti}_2\text{AlO}_{9-d}$  (Ln=La, Nd; A=Ca, Sr). Introduction of cation and oxide ion vacancies causes expansion of the perovskite lattice and enhancement of electrical conductivity. The  $P_{\text{O}_2}$  dependence of the conductivity and the ionic transference numbers of  $\text{LaSr}_2\text{Ti}_2\text{AlO}_9$  and  $\text{LaSr}_{1.7}\text{Ti}_2\text{AlO}_{8.7}$  indicate that these

compounds are mixed conductor of electrons and oxide ions.

#### References

- [1] H. Yoshioka, S. Kikkawa (1998) : "Oxide ion conduction in A-site deficient La-Ti-Al-O perovskite", *J. Mater. Chem.*, **8**, 1821.
- [2] M. Kestigian, J. G. Dickinson, and R. Ward (1957) : "Ion-deficient phases in titanium and vanadium compounds of the perovskite-type", *J. Am. Chem. Soc.*, **79**, 5598.
- [3] H. P. Rooksby, E. A. D. White, and S. A. Langston (1965) : "Perovskite-type rare-earth niobates and tantalates", *J. Am. Ceram. Soc.*, **48**, 447.
- [4] L. Latie, G. Villenure, D. Conte, and G. L. Flem (1984) : "Ionic conductivity of oxides with general formula  $\text{Li}_x\text{Ln}_{1/3}\text{Nb}_{1-x}\text{Ta}_x\text{O}_3$  (Ln=La, Nd)", *J. Solid State Chem.*, **51**, 293.
- [5] Y. Inaguma, C. Liquan, M. Itoh, T. Nakamura, T. Uchida, H. Ikuta, and M. Wakihara (1993) : "High ionic conductivity in lithium lanthanum titanate", *Solid State Commun.*, **86**, 689.
- [6] F. Izumi and T. Ikeda (2000) : "A Rietveld-analysis program RIETAN-98 and its applications", *Mater. Sci. forum*, **321-324**, 198.
- [7] V. Thangadurai, G. N. Subbanna, A. K. Shukla and J. Gopalakrishnan (1996) : " $\text{AM}_{1-x}\text{Al}_x\text{O}_{3-x}$  (A=Na or K; M=Nb or Ta): New Anion-Deficient Perovskite Oxides Exhibiting Oxide Ion Conduction", *Chem. Mater.*, **8**, 1302.
- [8] R. D. Shannon (1976) : "Revised Effective Ionic Radii and Systematic Studies of Interatomic Distances in Halides and Chalcogenides", *Acta Crystallogr.*, **A32**, 751.
- [9] V. M. Goldschmidt (1926) : "Die Gesetze der Kristallochemie", *Naturwissenschaften*, **14**, 477.